Potential Dependent Ag Nanoparticle Electrodeposition on Vulcan XC-72R Carbon Support for Alkaline Oxygen Reduction Reaction

Melissa Vega-Cartagena,^{1*} Arnulfo Rojas-Pérez,¹ Guillermo S. Colón-Quintana,¹ Daniel A. Blasini Pérez,¹ Armando Peña-Duarte,^{1,2} Eduardo Larios-Rodríguez,^{1,3} Marco A. De Jesús,⁴ Carlos R. Cabrera^{1*}

ABSTRACT

Carbon-supported Ag nanocatalysts, synthesized at five different electrodeposition potentials ranging from 0.0 to 0.4 V vs. RHE, were successfully prepared by using the rotating disk slurry electrode (RoDSE) technique. This was done to determine the ideal electrodeposition parameters that facilitate optimal metal loading and particle dispersion for an efficient oxygen reduction reaction (ORR) through the 4-e⁻ pathway. In this study, the potentials were chosen based on different regions of Ag electrodeposition on a clean glassy carbon electrode. Each Ag/Vulcan catalyst was characterized using different techniques including TEM, XRD, ICP-OES, XPS, and Raman spectroscopy. These techniques confirmed the presence of Ag on the carbon support and determined that the applied potential affected the Ag oxidation state and catalytic ORR activity. Herein, we show that as the electrodeposition potential increases, we observe a lower electrodeposition current. This suggests gentle Ag deposition on the carbon support, resulting in reduced agglomeration. We confirm that the deposition potential of the Ag has a direct effect on the electrocatalytic behavior of the Ag/C catalyst. Ag crystallinity was determined using XRD, which showed a particle size in the range of 1 to 35 nm for each potential. ORR studies were conducted in O₂ saturated 0.1 M KOH solution using the rotating disk electrode (RDE) technique and cyclic voltammetry. The oxygen species at the Ag NPs surface suggest a synergistic effect in the ORR mechanism. Finally, among the five studied electrodeposition potentials of Ag. 0.1 V vs. RHE provided the optimal conditions to generate Ag catalysts with low agglomeration, small particle size, high ORR mass activity, and electron transfer equal to 3.5 in 0.1 M KOH electrolyte.

KEYWORDS: Oxygen reduction reaction, Vulcan XC-72R, silver, nanoparticles, RoDSE

¹ PREM Center for Interfacial Electrochemistry of Energy Materials and Department of Chemistry, Molecular Sciences Research Center, University of Puerto Rico, Río Piedras Campus, San Juan, PR 00925-2537

² Department of Physics, University of Puerto Rico, Río Piedras Campus, San Juan, PR 00925-2537

³ Departamento de Ingeniería Química y Metalurgia, Universidad de Sonora, Hermosillo, México 83000

⁴ Department of Chemistry, University of Puerto Rico, Mayagüez Campus, Mayagüez, PR 00680

^{*} Corresponding authors: melissa.vega@upr.edu; carlos.cabrera2@upr.edu

Introduction

World energy demands are one of the key challenges in modern times, as 80 percent of all energy production is still derived from non-renewable resources such as petroleum, coal, and natural gas. These sources are responsible for the generation of carbon dioxide and other greenhouse gases that contribute to pollution and global warming. Despite these, renewable energy consumption has increased in recent years.³ The successful implementation of renewable energy technologies will enable a clean, greenhouse gas-free economy.² Fuel cells in particular are noteworthy due to their ability to produce electricity from chemicals via electrochemical reactions.⁴ In recent years, alkaline fuel cells (AFCs) have competed with solid electrolyte fuel cells such as PEMFCs. AFCs can reach electrical efficiency of up to 70 percent, are usable in open conditions, and demonstrate excellent oxygen kinetics and ohmic polarization at low current densities, leading to faster oxygen reduction reaction (ORR) rates than in the typical acidic media of PEMFCs. Also, AFCs show longer longevity due to a less corrosive environment compared to acidic medium.5, 6 ORR limiting factors at a fuel cell's cathode come from its slow kinetics and the ORR competing pathways: the reduction of O₂ to H₂O proceeding via a 4-electron or a 2-electron reduction, with hydrogen peroxide (H2O2) as an intermediate. In response to these limitations, a variety of catalysts for the ORR in alkaline media have been explored. Current research has consistently shown that noble metals, such as Pt, Ag, Pd, Au¹⁰ and Ir¹¹ are the best catalysts for this reaction. Among all these precious metals, Pt is considered the benchmark in both acidic and alkaline media.^{7, 12-14} Unfortunately, Pt is both rare and highly expensive, making it impractical for widespread commercial applications. ¹⁴ In contrast, Ag is considered a potential alternative to Pt for ORR in alkaline fuel cells, due to its high activity and being a much more cost effective metal.^{8, 13, 15} In particular, Ag can proceed via a 2 or 4-electron pathway depending on different factors such as electrode potential applied, oxidation, and surface states. ¹⁶

Fewer studies have been done on dispersed Ag nanoparticles (NPs) in alkaline media, as compared to other precious metals.⁷ Significant challenges faced by Ag NPs as an ORR catalyst include the agglomeration of NPs due to high surface energy and the need to fine-tune the particle size in order to obtain good catalytic activity. 12, 17 This requires the design and testing of improved synthesis methods that help to customize and effectively control the Ag NP size and dispersion for better ORR catalysis. Several different methods have been reported for Ag nanoparticle synthesis, however, the Rotating-Disk Slurry Electrodeposition Technique (RoDSE), developed by Santiago et al. 18, is the main contender for the synthesis of carbon-supported nanoparticles. The RoDSE technique consists of the electrodeposition of a metal onto a desired support surface, mainly carbon supports. Vega et al.⁸ reported that pure silver was deposited on Vulcan XC-72R using the RoDSE technique and tested for ORR performance.⁸ Vulcan XC-72R is a commonly used NP support due to several main advantages over other carbon supports, while being easier to obtain than other materials and at a lower cost. 19 In this work, Ag NPs were synthesized and electrochemically deposited onto a Vulcan XC-72R carbon support using the RoDSE technique in acidic media. Several different nanocatalyst samples were prepared by varying the electrodeposition potentials versus RHE in a range from 0.0 V to 0.4 V vs. RHE. This was done in order to determine the optimal Ag electrodeposition parameters that guarantee ideal metal loading and particle dispersion to carry on an efficient ORR through a 4-electron pathway.

EXPERIMENTAL SECTION

Catalyst Preparation

Ag was electrodeposited on Vulcan XC-72R using the RoDSE technique following the conditions previously reported by *Vega et al.*⁸ Reference [18] provides a representative schematic and complete details about the RoDSE technique. Herein, the working electrode consisted of a glassy carbon (GC) disk (PINE Research Instrument Company), with a 5 mm diameter set to rotate at 2000 rpm in the slurry solution using a modulated speed rotator (MSR, PINE Research Instrument Company). A reversible hydrogen electrode (RHE) and a Pt wire were used as reference and counter electrodes, respectively. In all three compartments, aqueous sulfuric acid solution (0.1 M) was added as supporting electrolyte.

Each Ag/Vulcan XC-72R catalyst electrodeposition was done by applying one of five different constant reductive potentials, ranging from 0.0 V to 0.4 V vs. RHE. The reductive potential was applied after the addition of each of the 12 aliquots of Ag metal salt precursor solution, consisting of 1.23 mL of 5 mM AgNO₃ (Sigma Aldrich) at 20 min intervals, to the working electrode compartment, for a total electrodeposition time of 240 minutes. Finally, when the RoDSE electrodeposition was completed, we followed the previously reported procedure by *Vega et al.*⁸ Commercial E-TEK 20 wt.% Pt/Vulcan XC-72R was used for comparison.

Physical Characterization

Transmission Electron Microscopy (TEM). TEM was performed on a FEI Tecnai G2F20 TEM/STEM microscope operated at 200 kV to obtain information about the morphologies of the catalysts. The carbon-supported catalysts were deposited on a 200-mesh lacey carbon copper grid. Particle size histogram was determined using MIPAR software utilizing different regions of the carbon copper grid to obtain a representative perspective of each catalyst average particle size.

X-ray diffraction (XRD). XRD patterns were recorded for the RoDSE synthesized Ag/Vulcan catalyst powders with a Rigaku Ultima IV X-ray diffractometer and using Cu K α radiation (λ =1.54 Å). The 20 angular range was scanned and explored in a range from 10° to 90° at a scan rate of 3°/min and 0.02° steps.

X-ray photoelectron spectroscopy (XPS). XPS spectra were determined by means of a PHI 5600ci spectrometer, with an Al K α polychromatic X-ray source of 350 W settled at 45° and a hemispherical electron energy analyzer. Vacuum chamber pressure was below $9x10^{-9}$ mbar. Carbon tapes were used as adhesive support of small quantities of the Ag-based catalytic powder. Ag 3d and C 1s XPS spectra were deconvoluted and analyzed using the Multipack Physical Electronics curve-fitting program. A C 1s peak at 284.5 eV was applied to correct for binding energy shifts of the reported binding energies.

Raman spectroscopy. Raman analysis was done using an Xplora confocal Raman (Horiba Scientific, Co.), an Olympus BX-51 microscope, and a 10X objective in backscattering configuration. Spectra were acquired using 600 grooves/mm grating size and an average of 24 sampled spectra with a 5 second irradiation of the 532 nm line at 30 mW laser power.

Induced Coupled Plasma–Optical Emission Spectrometry (ICP–OES). Ag/Vulcan catalyst loadings were determined using an Optima 8000 Perkin Elmer ICP-OES with standard plasma parameters. Herein, an approximate 15 mg of each sample was processed following the ASTM D3174 method for the obtention of ashes. Then, ashes were digested with 10 mL concentrated HNO3 and heated until 1 mL remained. The solutions were passed through Whatman glass microfiber filters (GF / F grade) and reconstituted with 2% HNO3 solution. Quantification of all samples was carried out using a calibration curve.

Electrochemical characterization

The catalyst inks consisted of 1 mg of catalyst powder mixed with 140 μ L of ethanol (99.5% Sigma Aldrich) and 10 μ L of Nafion solution (5% solution in alcohol, Sigma Aldrich). The GC electrode was modified by adding 2.75 μ L of the black ink and then air-dried at room temperature for 30 min. This modified electrode was then cycled in Ar-purged electrolyte 0.1 M KOH solution at a potential window between 0.4 and 1.5 V vs RHE at a potential scan rate of 25 mV s⁻¹ until a reliable and reproducible voltammogram was obtained for each catalyst.

Linear sweep voltammetry (LSV) measurements were done using a catalyst ink-modified glassy carbon rotating disk electrode in an oxygen-saturated 0.1 M KOH solution and the data was recorded in the negative directional potential sweep from 1.00 to 0.00 V vs RHE, at a scan rate of 5 mV/s. The electrode rotation speed was varied from 400 to 2500 rpm. The electrochemical characterization of the different Ag/Vulcan catalysts was performed using a three-electrode SP-50 potentiostat/galvanostat (Biologic Instruments).

The rotating disk electrode (RDE) system was used to for synthesis of all catalyst samples and also for the oxygen reduction reaction studies in alkaline media. ORR analysis was done in O₂-saturated 0.1 M KOH. In addition, cyclic voltammetry (CV) was done to evaluate the electrochemical behavior of each Ag/Vulcan XC-72R catalyst and to identify the Ag oxidation and reduction peaks. Before each experiment, the GCE was carefully polished to a mirror finish with alumina powder gradient ranging from 1.0 to $0.05\mu m$ (Buehler Micropolish). In this work, the current densities were normalized using the geometrical area of the glassy carbon electrodes.

Results and Discussion

Ag Electrodeposition

Cyclic voltammetry was done using a clean GCE in a 5 mM AgNO₃ in Ar-saturated solution at a scan rate of 20 mV s⁻¹(see Figure 1). A starting potential of 1.4 V vs. RHE was chosen to make sure that the Ag⁺ cations were in solution. In the first scan, we observed a cathodic peak near 0.85 V vs. RHE,

corresponding to the deposition of Ag onto the GCE surface. When the Ag catalysts were scanned to positive potentials in the potential range of 0.80 to 1.0 V vs. RHE, we observed a unique cathodic peak for all studied catalysts, which agrees well with results reported in literature.^{5,11} The anodic contributions from 0.6 to 0.8 V vs. RHE can be attributed to the formation of an Ag₂O layer,¹¹ while the cathodic peak centered at 0.9 V vs. RHE is associated with the oxide reduction to metallic silver.^{11,20}

For each cycle, a distinct Ag voltammogram was observed with higher current densities due to the Ag deposition on every cycle. According to the data shown in **Figure 1**, five different reduction electrodeposition potentials (0.0 V, 0.1 V, 0.2 V, 0.3 V and 0.4 V vs. RHE) were chosen for the electrodeposition of Ag on the carbon Vulcan support using the RoDSE method.

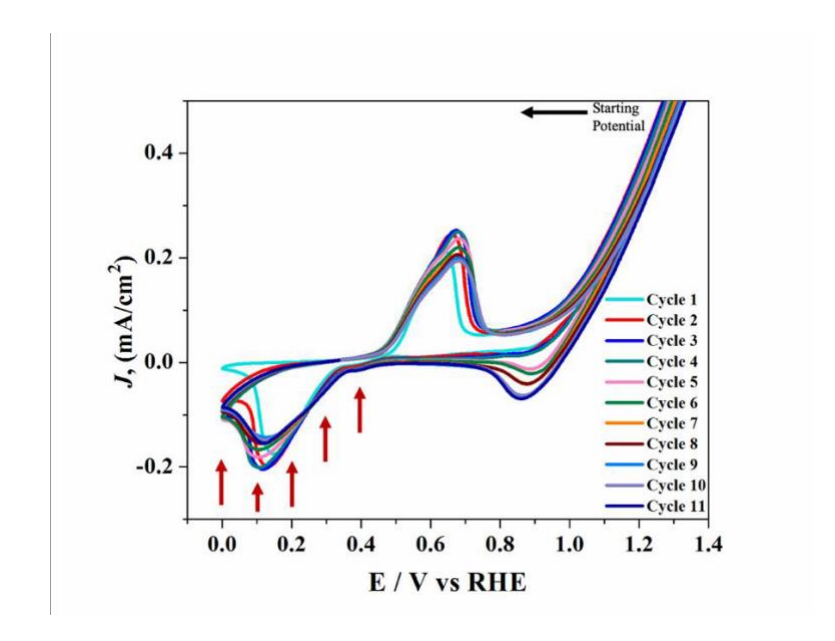


Figure 1. Cyclic voltammograms of a GCE in a 5 mM AgNO3 and 0.1 M KOH in Ar-saturated at a scan rate of 20 mV/s. The arrows indicate the different RoDSE Ag electrodeposition potential.

Surface Characterization

TEM images of all electrodeposited Ag catalysts synthesized at various reduction potentials are presented in **Figure 2**. These images show different particle sizes and dispersion for each Ag electrodeposition potential applied. Ag particles deposited at 0.0 V vs RHE showed a strong tendency to agglomerate. At this potential, Ag particles of 2 nm in size were observed, but most were smaller than 1 nm. A large amount of Ag was reduced and the support was not enough to disperse the particles, suggesting that these Ag particles in the sample were agglomerated. However, as the value of the reduction potential increased (0.1 V vs. RHE), we observed Ag NPs frequently and of larger size (7.5 nm). For Ag particles deposited at 0.2 and 0.3 V vs. RHE, Ag particles homogeneously dispersed on the carbon support with an approximate diameter particle sizes below 15 nm were observed in the TEM images. This indicates that the carbon substrate contributes enough surface area for the dispersion of the Ag NPs. In the final applied potential under study, i.e. 0.4 V vs. RHE, fewer Ag particles were observed, but with good dispersion and

with different sizes up to 35 nm. Due to the slower kinetics of particle formation we obtain bigger Ag particle size, which suggest that initially there is no gradient of Ag⁺ cations and the quantity of Ag ion-near the surface is large enough, which allows the formation of agglomerates. The particles synthesized in this study are significantly smaller than those reported previously in the literature. These results were found to be in good agreement to the data with the results obtained in the electrodeposition process. At a more negative electrodeposition potential (0.0 V vs. RHE), a higher deposition current was obtained. This indicates that Ag was being deposited in a way that resulted in agglomeration and less particle dispersion. The electrodeposition potential showed an inverse relationship with deposition current: as the potential increased up to 0.4 V vs RHE, the current decreased, resulting in the gentle deposition of Ag and less agglomeration.

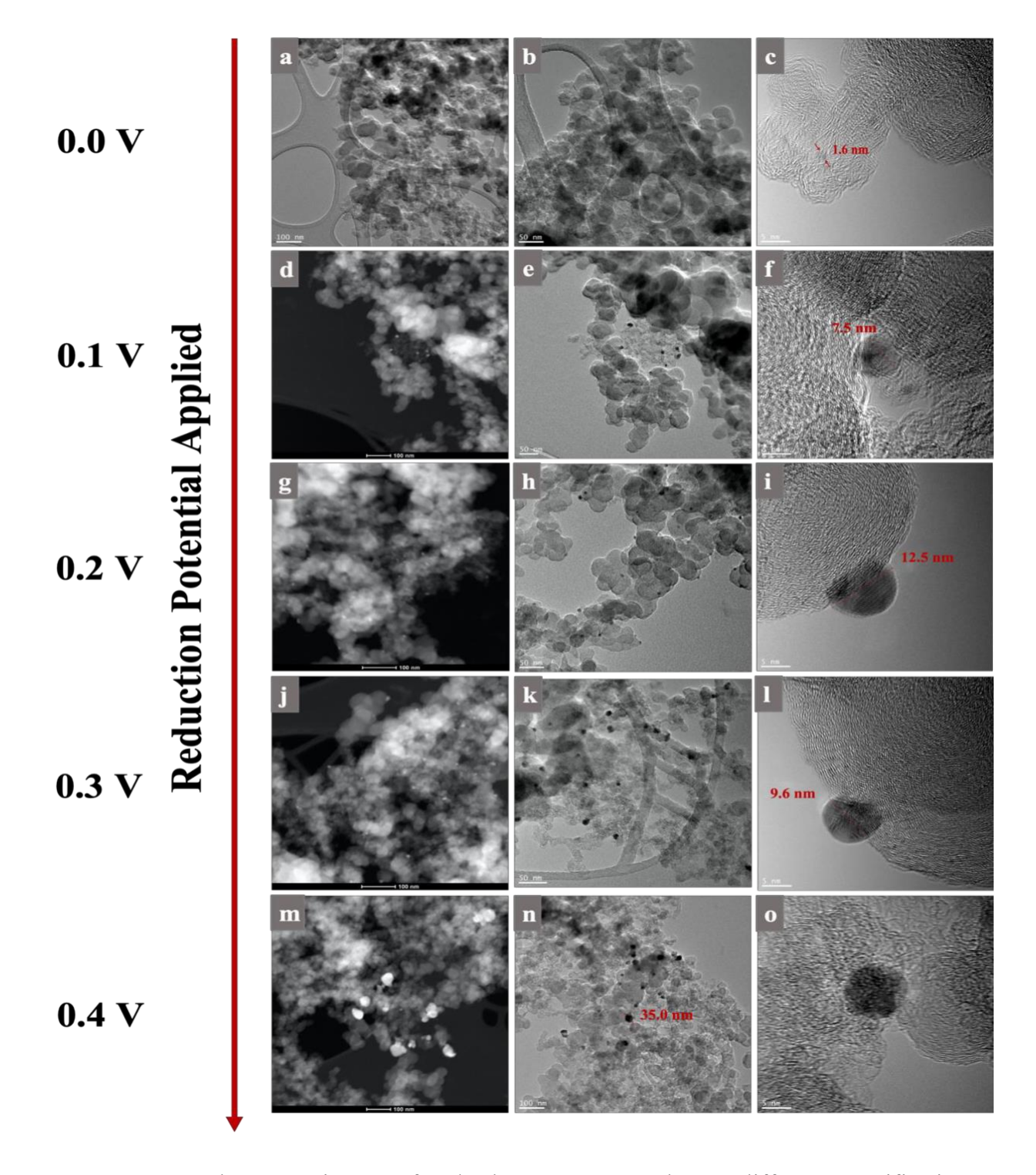


Figure 2. TEM and HRTEM images of Ag/Vulcan XC-72R catalysts at different magnifications, prepared by RoDSE: images of Ag/Vulcan catalyst at (a) (scale: 1000 nm), (b) (50 nm) and (c) (5 nm); (d) (100 nm), (e) (50 nm) and (f) (5 nm); (g) (100 nm), (h) (50 nm) and (I) (5 nm); (j) (100 nm), (k) (50 nm) and (l) (5 nm); and (m) (100 nm), (n) (100 nm) and (o) (5 nm), were done at 0.0 V, 0.1 V, 0.2 V, 0.3 V, and 0.4 V vs. RHE, respectively.

TEM image analysis and the fast Fourier transform (FFT) are shown in **Figure 3** for the Ag/Vulcan catalysts synthesized at 0.2, 0.3 and Ag 0.4 V vs. RHE. For the potentials of 0.0 and 0.1 V, the analysis could not be analyzed as the suitable size required, in order to do this procedure, were not found.

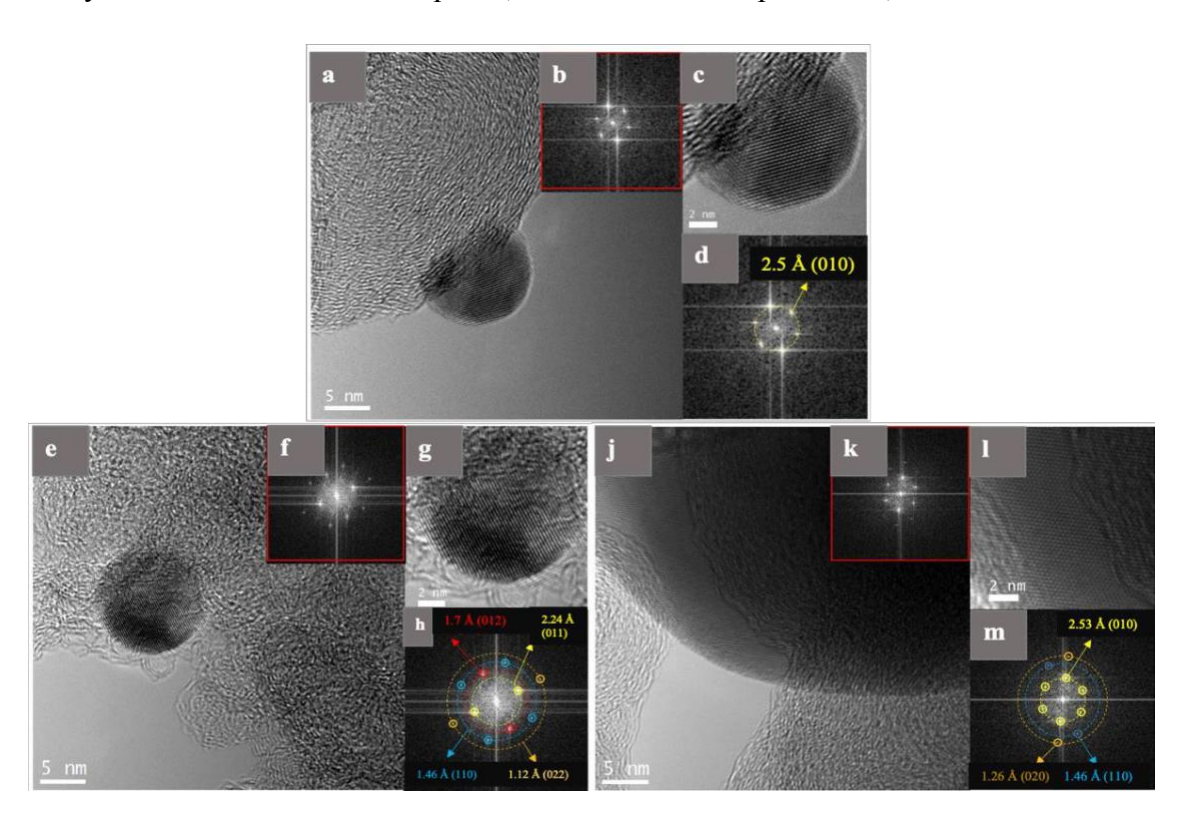


Figure 3. TEM images and the FFT analysis of Ag/Vulcan prepared by RoDSE at 0.2 V (a,b,c and d), 0.3 V (e,f,g and h) and 0.4 V (j,k,l and m) vs. RHE.

Figures 3 shows the spacing of 2.5, 2.24, 1.74, 1.46, 1.26 and 1.12 Å corresponding to the planes (010), (011), (012), (110), (020) and (022), respectively. These spacings correspond to the hexagonal structure of the Ag. **Figure 3a and 3c** shows Ag NPs supported on the carbon support synthesized at 0.2 V, the insert (b) shows the FFT of the TEM image shown in **Figure 3c**. In **Figure 3d**, the spots corresponding to the inter-planar spacings are labeled as (010) with a diameter of 2.5 Å. **Figure 3e** shows a Ag/Vulcan synthetized at 0.3 V, the insert (k) shows the FFT of the area shown in **Figure 3g**. **In figure 3h**, the spots corresponding to the spaces are labeled interplanes 2.24, 1.74, 1.46 and 1.12 Å which corresponds to the planes (011), (012), (110) and (022), respectively. **Figure 3j** presents Ag/Vulcan synthetized at 0.4 V, the insert (k) shows the FFT of area in **Figure 3l**. In **Figure 3m**, the spots corresponding to the spaces are labeled interplanes 2.5, 1.46 and 1.26 Å, which corresponds to the planes (010), (110) and (020), respectively. The three analyzed samples at 0.2 V, Ag 0.3 V, and Ag 0.4 V show the interplanar spacings of the hexagonal Ag planes.

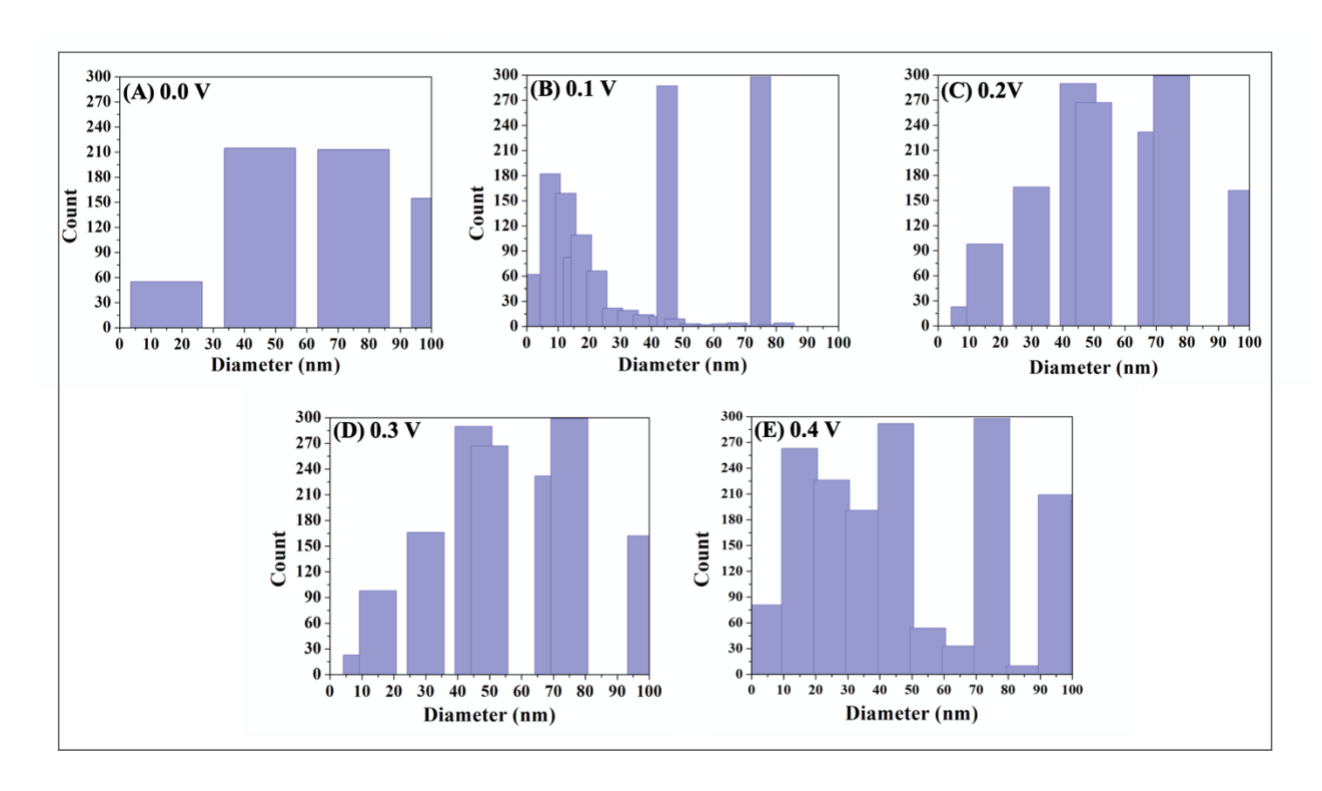


Figure 4. Particle size histogram of TEMs in Figure 2, in nanometers, from TEM images for Ag/Vulcan catalysts prepared by RoDSE at (A) 0.0 V, (B) 0.1 V, (C) 0.2 V, (D) 0.3 V and (E) 0.4 V vs. RHE.

The particle size histograms are shown in **Figure 4** and demonstrate the tendency of particle agglomeration as the reduction potential varied and rpms increased. The applied potentials of 0.2 V and 0.3 V vs. RHE showed the most uniform distribution of particle agglomeration. The increase of Ag deposition intensity with the shift of potential to more negative potentials can explain the increase of Ag particles agglomeration level.

Physicochemical Analysis

The crystalline structure of five different Ag/Vulcan catalysts prepared with different reduction potentials were further characterized by XRD and are shown in **Figure 5.** The broad peak located at ~25° is attributed to the (200) crystalline plane of the Vulcan XC–72R nanoflakes. The peak at 38°, in the XRD pattern, is for Ag (111) with the highest contribution of Ag crystal facets. In addition, the peaks located at 44.1°, 64.4°, 77.3°, and 83.4° are attributed to Bragg reflections on the (200), (220), (311), and (222) crystal planes of Ag, with a face-centered cubic (FCC) structure. Here, the XRD pattern not only shows the diffraction indexes of Ag, but also presents a minor characteristic peak of Ag₂O at around 34.2° (see **Figure 5B).** The generation of Ag₂O in the catalyst can be explained by the smaller Ag NPs in the Ag/Vulcan XC-72R support, which expose more Ag atoms on the carbon surface to be oxidized by the oxygenic groups. However, this indicates that most of the Ag in the different catalyst is in the metallic form. For further analysis, Scherrer's equation was employed and the average crystallite sizes of Ag particles were calculated to be in a range of 1.5 to 31.7 nm.

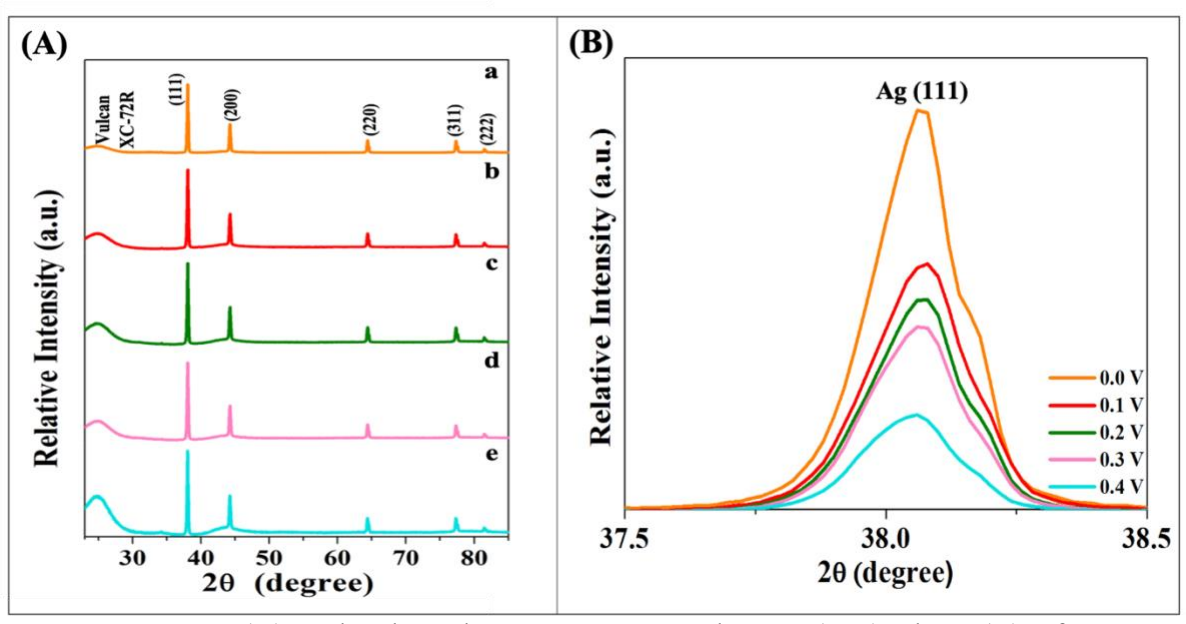


Figure 5. XRD patterns (A) and enlarged XRD spectra at the Ag (111) plane (B) of as-prepared Ag/Vulcan XC-72R samples synthesized by RoDSE at (a) 0.0 V, (b) 0.1 V, (c) 0.2 V, (d) 0.3 V and (e) 0.4 V vs. RHE.

The effect of the applied potential on the catalyst surface chemical composition was evaluated by XPS analysis. **Table S1 and Figure S1** shows the full half-maximum width (FHMW) of Ag 3ds/2 and Ag 3ds/2 and C 1s binding energy analysis of the XPS measurements for each RoDSE applied potential. The XPS binding energy spectra for Ag 3d and C 1s (**Figure S1**), obtained for the synthesized samples, were deconvoluted and analyzed using the Multipack Physical Electronics curve-fitting program. A C 1s peak at 284.5 eV was applied to correct energy shifts of the binding energies reported. All spectra samples exhibited a minimal Ag 3d binding energy peak signal, i.e. low signal to noise level.²¹ The abundance of Vulcan XC-72R support may block the 3p and 3d metallic (Ag) photoelectrons.^{9, 22}

Since the presence of Ag was determined and confirmed by CV, XRD, and ICP-OES, the Ag 3d peaks were fitted to evaluate Ag metallic and Ag oxide species peaks. The peak assignments for the Ag 3d components are reported in **Table 1.** The Ag 3d5/2 and Ag 3d3/2 binding energy peaks assignments were 368.4 and 374.4 eV, respectively. Ag transition energies and the 6eV spin-orbit splitting of the 3d doublet are characteristic energies of Ag in the metallic form. ^{20, 23} The peak assignments for the Ag 3d binding energy peak components for Ag oxide species (Ag2O and AgO) were 368.1 and 367.6 eV and 374.1 and 373.6 eV for Ag 3d5/2 and Ag 3d3/2, respectively. ²⁰ After curve fitting all the components, the peak deconvolution was developed as shown in **Table 2.**

Table 1. X-ray photoelectron spectroscopy Ag 3d binding energy peak assignments.

Silver 3d Components	Binding Energy (eV)		
	Agd _{5/2}	Agd _{3/2} (Δ=6eV)	
Ag	368.4	374.4	
Ag_2O	368.1	374.1	
AgO	367.6	373.6	

Table 2. Ag 3d components for X-ray photoelectron spectroscopy binding energy peak deconvolution.

Sample (V)	Binding Energy (eV)				
	Ag ⁰		Ag ^{+/++}		
	$\mathbf{Agd}_{5/2}$	Agd _{3/2} (Δ=6eV)	$\mathbf{Agd}_{5/2}$	$\mathbf{Agd}_{3/2}(\Delta=6\mathrm{eV})$	
	(368.3 eV)	(374.3 eV)		(374.3 eV)	
0.0	368.7	374.7	368.3	374.3	
0.1	368.7	374.7	368.4	374.4	
0.2	368.5	374.5	367.3	373.3	
0.3	368.7	374.7	368.2	374.2	
0.4	368.6	374.6	368.3	374.3	

Because Ag particles are on the nanometer scale, the oxidation state of the metallic NPs will reflect the bulk oxidation state.²² The Ag/C catalyst oxidation states were determined by XPS binding energy peak deconvolution analysis. The contribution of each Ag component was summarized in **Table 3.**

Table 3. Contribution of the oxidation state of Ag 3d_{5/2} and Ag 3d_{3/2} binding energy components for each Ag/Vulcan XC-72R catalyst synthesized.

	%Contribution (Total Area = $Ag^0d_{5/2} + Ag^{+/++}d_{5/2}$			Total %Area		
Sample (V)	Ag ⁰		$\mathbf{A}\mathbf{g}^{ ext{+/++}}$		d _{5/2}	d _{3/2}
	Agd _{5/2} (368.3 eV)	Agd _{3/2} (Δ=6eV) (374.3 eV)	$\mathbf{Agd}_{5/2}$	Agd _{3/2} (Δ=6eV) (374.3 eV)	$\mathbf{A}\mathbf{g}^0 + \mathbf{A}\mathbf{g}^{+/++}$	$\mathbf{A}\mathbf{g}^0 + \mathbf{A}\mathbf{g}^{+/++}$
0.0	81.6	81.8	18.4	18.2	100.0	100.0
0.1	15.6	15.0	84.4	85.0	100.0	100.0
0.2	87.5	87.5	12.5	12.5	100.0	100.0
0.3	69.2	71.1	30.8	29.0	100.0	100.0
0.4	56.1	55.3	43.9	44.7	100.0	100.0

For all the Ag/Vulcan XC-72R samples, the quantities and physical regions analyzed, the silver:silver-oxide (A^0 :Ag^{+/++}) ratio relation was set by open circuit potential during the RoDSE technique. The Ag 3d XPS binding energy peaks show that the quantity of Ag deposited on the synthetic catalyst is affected by the electrodeposition potential.

To understand the chemical state of the Ag species, a detailed deconvolution of the Ag(3d) peak was performed. **Table S1** shows the Ag 3d binding energy signal consisted of a pair of doublets Ag 3ds/2 and Ag 3ds/2. The first doublet is attributed to metallic Ag and the second pair of peaks, shifted 6 eV to a lower binding energy, and is related to the Ag⁺ and Ag⁺⁺ chemical states as Ag₂O, AgO, and Ag(OH). In this sense, after a Shirley background subtraction, the Ag (3ds/2) peak was deconvoluted via Voigt profile analysis into two Gaussian-Lorentzian components, with similar full width at half maximum (FWHM). Based on this deconvolution analysis, 82, 16, 88, 70, and 56 % of the Ag was in the Ag⁰ (metallic) state, for samples synthesized at 0.0, 0.1, 0.2, 0.3 and 0.4 V vs. RHE, respectively. Meanwhile 18, 85, 12, 30 and 44 % was in the Ag^{+/++} chemical state, for applied potentials of 0.0, 0.1, 0.2, 0.3 and 0.4 V vs. RHE, respectively. The X² values were lower than 6 units for the whole analysis. It is necessary to emphasize that samples obtained at 0.1 V vs. RHE had the highest concentration of silver oxide (85%), while samples obtained at 0.2 V had main concentrations of metallic Ag (88%). Samples obtained at 0.4 V have a proportion of 56:44 for A⁰:Ag^{+/++} ratio, which suggests a near even distribution of Ag⁰ and silver oxide species.

Raman spectroscopy has been used as a tool to assess structural changes of sp² carbons and the charge transfer effects of allotropic forms of carbon and carbon clusters such as graphite, graphene, and

graphene oxides. ^{12, 20, 23-31} Several studies have demonstrated that Vulcan XC-72R has physicochemical characteristics similar to those of graphite, describing it as an amorphous mesoporous graphitic material. ^{12, 20} Vibrational analysis shows two bands at 1556 (±10) and 1356 (±20) cm⁻¹, corresponding to the characteristic G and D vibrations of carbon (**Figure 6A**). ²³ The G vibration is characteristic of inplane stretching vibration of sp²-hybridized carbon-carbon bonds, whereas D vibration occurs as a result of the structural disorder of the carbon atoms. ²⁴ Current research shows that G band shifts to lower frequencies upon addition of Ag to graphene oxide. ^{24, 32} Previous studies conducted by Vega *et al.* ⁸ report the untreated Vulcan G band at 1603 cm⁻¹. The intensity ratios of D and G bands (ID/IG) are another factor used to assess structural changes and metallic interactions on carbon substrates such as Vulcan. Vega *et al.* ⁸ reported a 1.1 ID/IG ratio for native Vulcan. In this work, the ID/IG ratios observed for Ag/Vulcan were 0.65, 0.66, 0.87, 1.21, and 0.61 at 0.0 V, 0.1 V, 0.2 V, 0.3 V, and 0.4 V vs. RHE, respectively (**Figure 6B**). Intensity changes in the carbon G band provide information on changes in carbon particle distribution within the Vulcan clusters, because of the chemical reduction processes. As expected, the intensity of the 0.2 V G band decreased, along with a large shift to low wavenumbers (-60 cm⁻¹) which indicates a more effective reduction on the Ag/Vulcan.

Figure 7 shows that for the present study, the signal shifted from -40cm⁻¹ to 60 cm⁻¹, at the 0.0 to 0.4 V vs. RHE range which brings it closer to that observed for a graphite lead (1564 cm⁻¹). This shift is indicative of a charge transfer effect between Vulcan and Ag and is reflected as a decreased bond order of the sp² carbons. This is indicative of the reduction conditions of the preparation of the catalyst and the incorporation of Ag onto the Vulcan material. The best RoDSE Ag/Vulcan condition at 0.2 V also showed a shift of the D-band to higher wavenumbers (1350 cm⁻¹), indicating conformational changes on the aromatic ring. These changes are indicative of a more uniform distribution of the metal catalyst within the Vulcan.

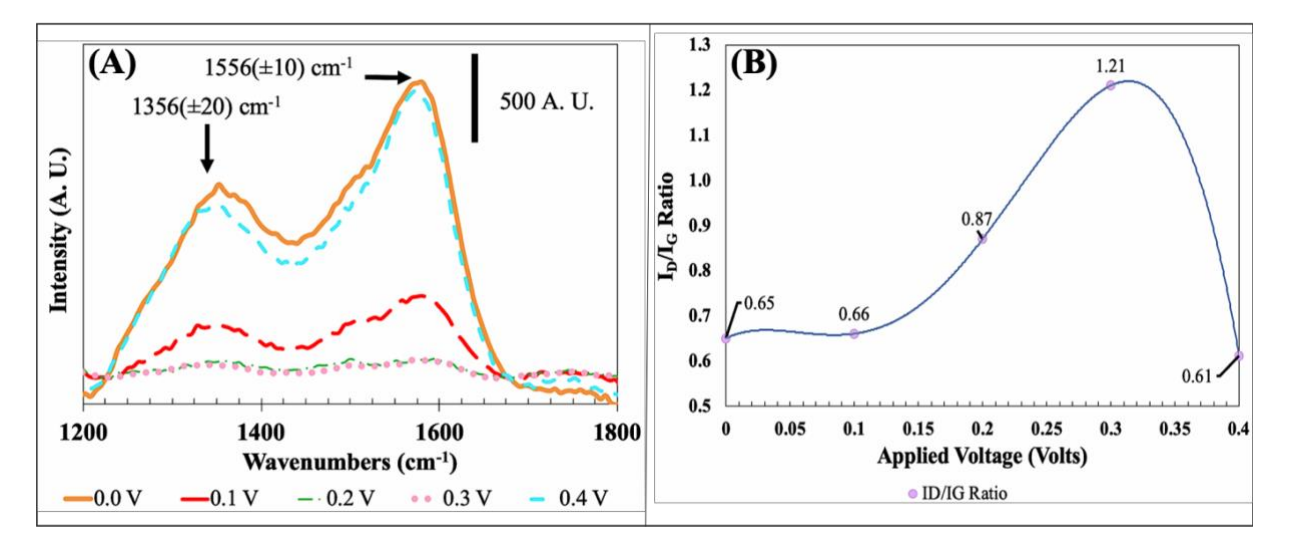


Figure 6. (A) Raman spectra and (B) intensity ratios of D and G Raman bands as function of the applied RoDSE potential vs. RHE for the synthesis of Ag/Vulcan XC-72R catalyst.

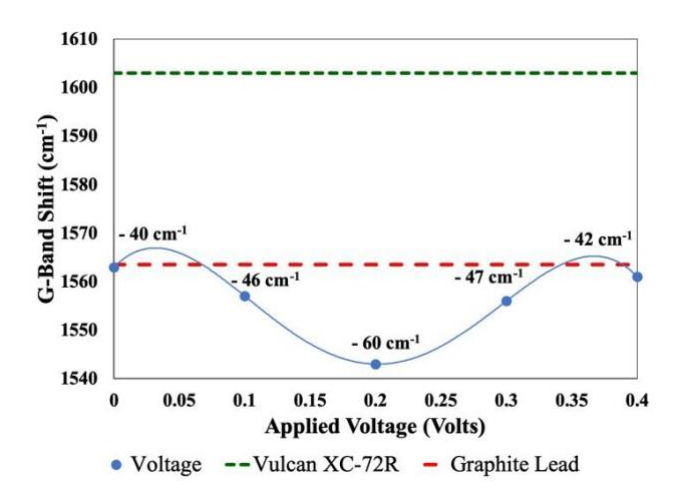


Figure 7. Changes in Ag/Vulcan G-Band Raman shift as function of the applied potential vs. RHE.

ICP-OES analyses were done to determine the amount of Ag deposited on Vulcan XC-72R at different RoDSE potentials. The Ag loadings (w/w%) are shown in **Table 4.** The percentages of Ag in the RoDSE catalyst were determined as followed: 4.74%, 4.99%, 7.1%, 2.98 % and 5.4%, for 0.0 V, 0.1 V, 0.2 V, 0.3 V and 0.4 V vs. RHE, respectively. The final catalyst metal loadings as determined by ICP are lower than those obtained in the chronoamperometry data (*vide infra*). These results demonstrate that as the applied potential became more positive, the mass of Ag deposited increased until it reached a maximum at 0.2 V. Then, Ag loading starts to decrease considerably at even more positive potentials. These results generally agree with the TEM results, in which it was challenging to find Ag particles deposited in the carbon support at the most positive potentials, including those examined at 0.0 V vs. RHE.

Table 4. ICP Ag characterization data

Potential (V vs RHE)	Ag concentration (% wt ± Std)	
0.0	4.74 ± 0.03	
0.1	4.99 ± 0.03	
0.2	7.1 ± 0.2	
0.3	2.98 ± 0.07	
0.4	5.4 ± 0.1	

Electrochemical Characterization

Figure 8 shows the electrodeposition chronoamperometry of Ag in 0.0 V, 0.1 V, 0.2 V, 0.3 V, and 0.4 V vs. RHE. This figure displays the cathodic currents obtained for each added aliquot of the precursor solution in deposition of Ag in each of the five electrodeposition potentials. We observe that the average deposition current decreased in relation to the more positive values of reduction potential applied due to lower faradaic yield in high overpotentials. The average maximum deposition cathodic current was -672 mA, -518 mA, -401 mA, -391 mA, and -313 mA for 0.0 V, 0.1 V, 0.2 V, 0.3 V, and 0.4 V vs. RHE, respectively. Nevertheless, it is important to mention the electrodeposition in a slurry may differ from the electrodeposition in solution, particularly because the presence of carbon flakes may result in the depolarization of Ag deposition.

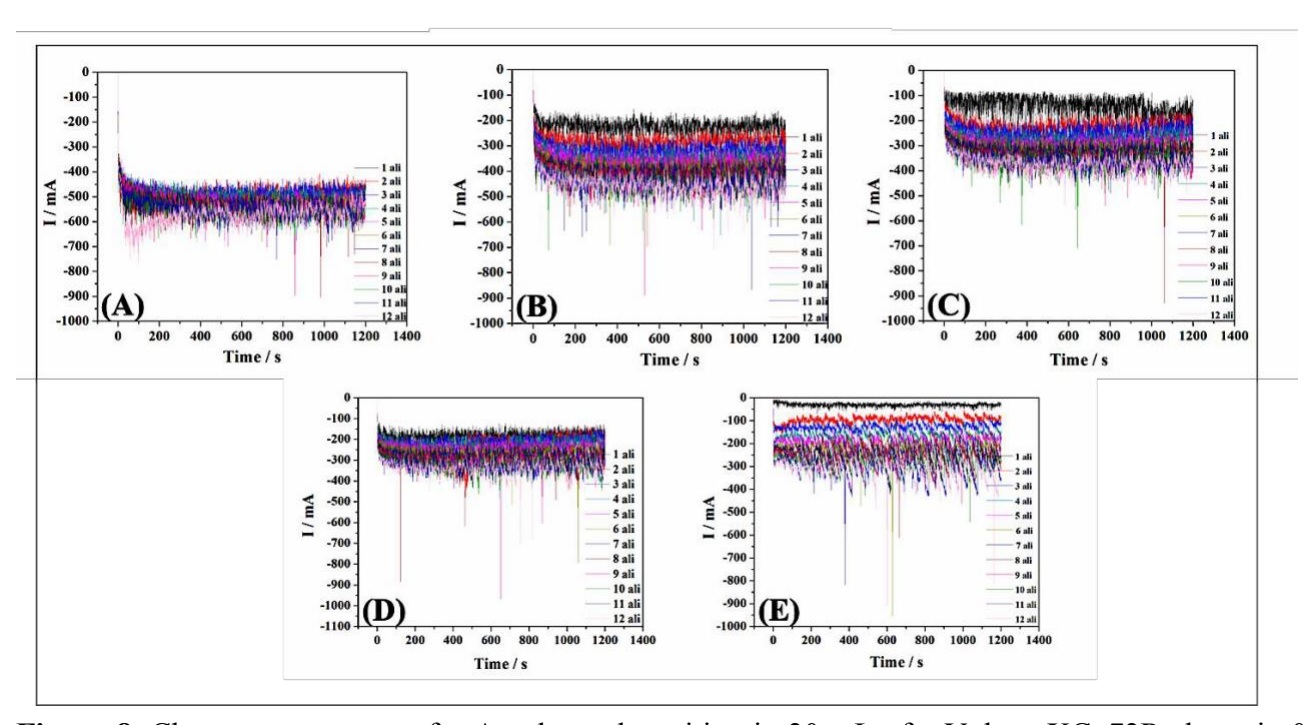


Figure 8. Chronoamperometry for Ag electrodeposition in 20 mL of a Vulcan XC–72R slurry in 0.1 M H2SO4 at different reduction applied potentials; (A) 0.0 V, (B) 0.1 V, (C) 0.2 V, (D) 0.3 V and (E) 0.4 V vs. RHE, respectively. For each applied potential, a total of twelve consecutive electrodepositions were added per 20-minute period. In each electrodeposition, a 1.23 mL aliquot of 5 mM of AgNO₃ was added to the slurry solution.

Figure S2 shows the chronoamperometry data results in combination with the chronoamperometry deposition profile using the RoDSE technique. Herein, the maximum percentages of both metals electrodeposited on the Vulcan slurry are 15 %, 12%, 9.5%, 9%, and 7.9% of Ag on Vulcan in 0.0 V, 0.1 V, 0.2 V, 0.3 V, and 0.4 V vs. RHE, respectively. The amounts of Ag electrodeposited are in good agreement with the TEM results reported above.

All electrochemically prepared catalysts using the RoDSE technique were characterized using CV. **Figure 9** shows the CV results of the as- prepared Ag/Vulcan catalysts with the five reduction potentials under study. At a scan rate of 25 mV/s, CV were done in an Ar-saturated 0.1 M KOH solution.

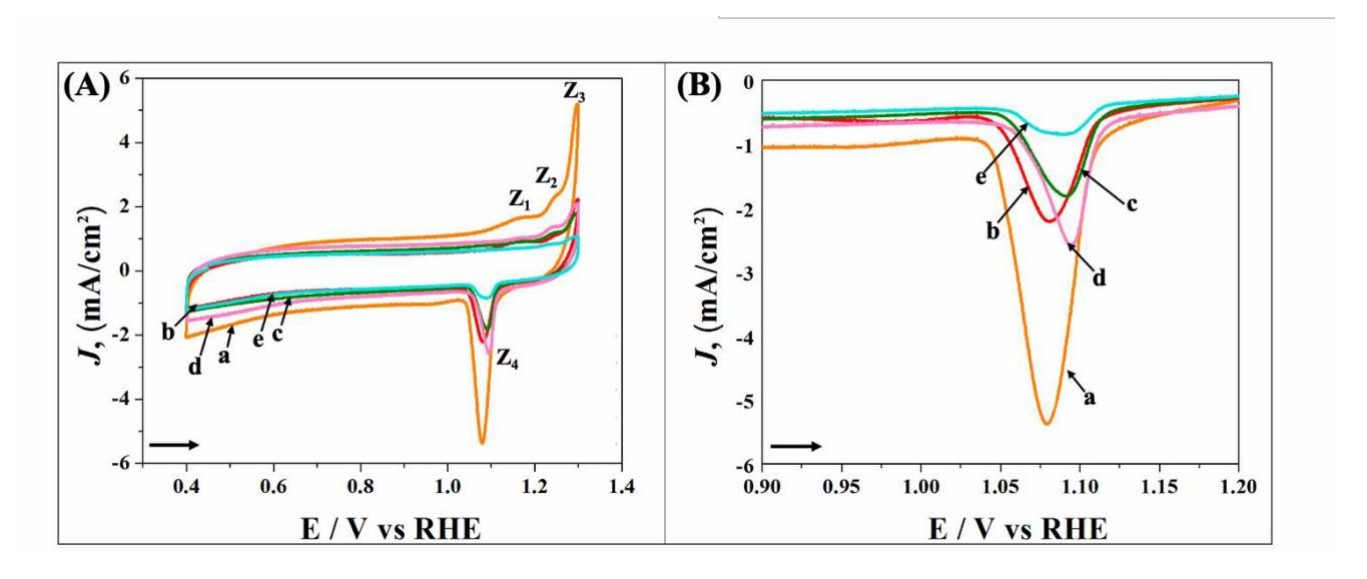


Figure 9. Cyclic voltammetry (A) and (B) and enlarged voltammogram at the Ag reduction peak (B) of the as-prepared samples synthesized by RoDSE at (a) 0.0 V, (b) 0.1 V, (c) 0.2 V, (d) 0.3 V, and (e) 0.4 V vs. RHE, respectively in Ar-saturated 0.1M KOH solution at a scan rate of 25 mV s⁻¹.

Three characteristic oxidation peaks developed when the Ag catalyst was scanned to positive potentials in the potential range of 1.10 to 1.30 V vs. RHE. These anodic peaks are designated as Z₁, Z₂, and Z₃, respectively, which are located at about 1.170, 1.238, and 1.296 V vs. RHE. Peak Z₁ is due to the Ag dissolution and the formation of a surface monolayer of Ag2O films, while peaks Z2 and Z3 are associated with the formation of bulk phases of silver hydroxide (AgOH) and silver oxide (Ag2O), respectively.²⁰ In previous studies, researchers report that the peak intensities of Z₁ have a direct correlation with the catalyst metal loadings. However, no correlation of peak intensities against the metal loading was found for peaks Z₂ and Z₃. These results coincide with CVs previously reported in the literature.²⁰ The CV of the Ag catalysts synthetized at the different reduction potential, all of them shows oxide reduction peaks, indicating that Ag is electroactive at the surface. The reduction of Ag2O is observed to be reversible on the negative scan, between 1.05 and 1.10 V vs. RHE (Figure 9), which is designated as Z4. However, the main difference with each CV data consists in the minor shifts in the reduction peak, Z4, to a positive potential with lower current which is directly related to the applied electrodeposition potential used to deposit Ag on carbon support. This observation can be explained by the arrangement and deposition of Ag at more positive electrodeposition potentials, and therefore by the larger carbon area available of Ag in contact with the electrolytic solution.

Figure 10 shows the ORR polarization curves obtained on the Ag/Vulcan catalysts at 0.1 M KOH solution. Here, steady-state polarization of the catalysts was performed at rotation speeds of 400, 900, 1200, 1600, and 2500 rpm, and results were recorded at a scan rate of 5 mV/s. A linear behavior can be observed between the limiting currents of the ORR and the rotation rate.

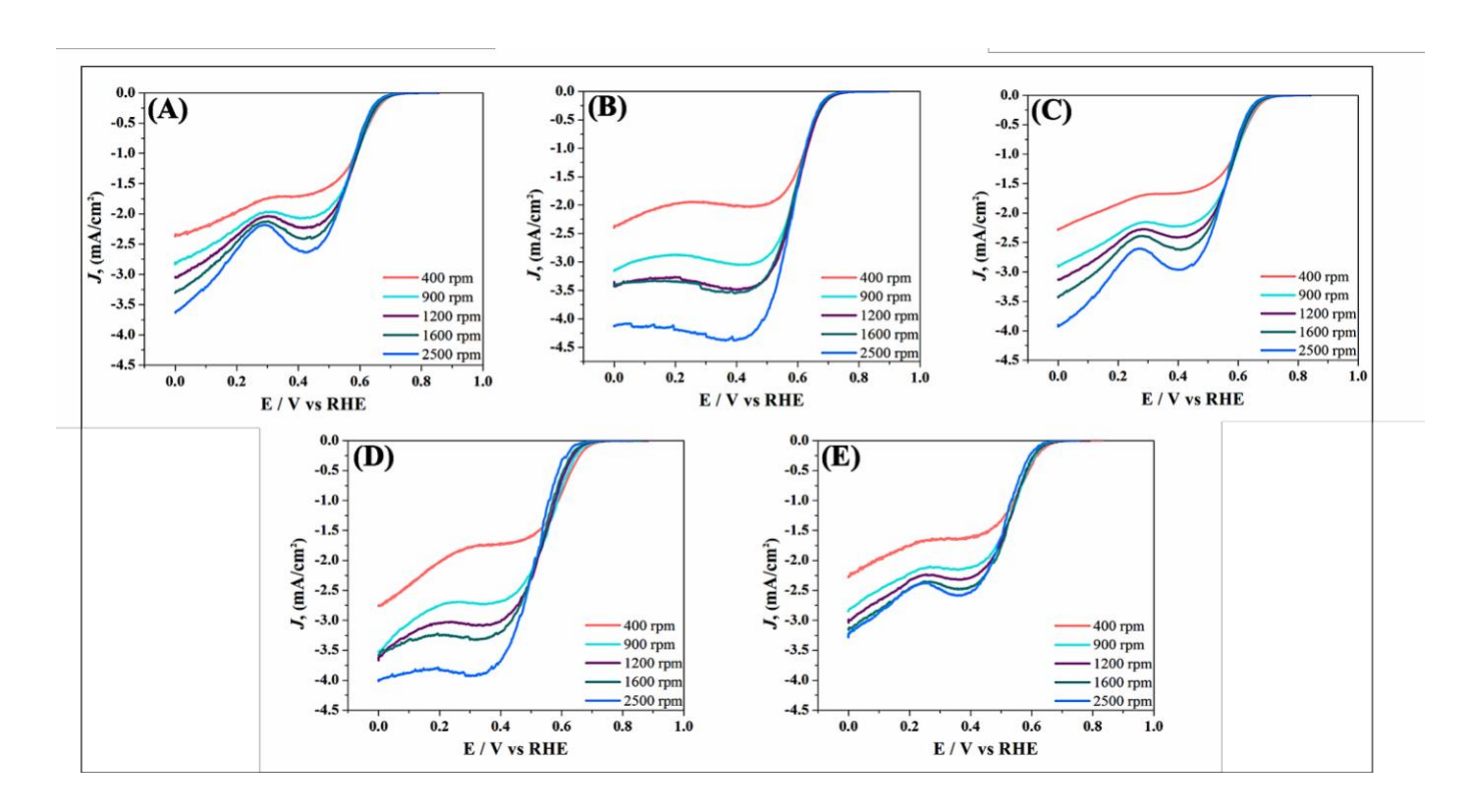


Figure 10. RDE voltammograms for electrochemically reduced Ag/Vulcan at 0.0 V (A), 0.1 V (B), 0.2 V (C), 0.3 V (D), and 0.4 V (E) vs. RHE in O₂-saturated 0.1 M KOH solution at a scan rate of 5 mV s⁻¹ a several rotation speeds; 400, 900, 1200, 1600, and 2500 rpm.

A comparison of RDE polarization curves for ORR on Ag/ Vulcan synthesized at the different reduction potentials and the benchmarks catalyst (Figure S3) in O2-saturated 0.1 M KOH solution is shown in Figure 11. Herein, we observed that all catalysts show considerably higher ORR activity than the bare GCE as the ORR E_{onset} and E_{1/2} shift to more positive values with the more negative electrodeposition potential (Figure S3). Notably, Ag NPs synthesized at 0.1 V vs. RHE exhibited dramatically higher ORR activity with more positive onset potential and higher currents than commercial Ag/C, while the Ag NPs synthesized at 0.0 V, 0.2 V, 0.3 V and 0.4 V vs. RHE displayed very poor ORR activity compared to the commercial Ag/C catalyst. In addition, we observed that each Ag/Vulcan catalyst demonstrates a different minimum current with each applied reduction potential. This could be related to a change in the reaction mechanism. These results are in agreement with TEM images, in which the results at 0.1 V have a small particle size with a high specific surface area, which provides more active sites, and uniform distribution of these sites for more efficient ORR. Despite the Ag NPs being synthetized using the same metal salt precursor, the different ORR activities demonstrate that the excellent ORR activity of Ag NPs did not originate from Ag by itself, but rather from the unique properties of synthesis using the RoDSE technique. These Ag NPs may combine with oxygen to form AgO2 and an oxygen complex due to spin accommodation.³³ The complex may have the effect of accelerating the adsorption of oxygen onto the electrode, which facilitate an easier ORR reaction.³³ The results obtained in this study are in agreement with the XPS results reported above (Table 3), in which the Ag/Vulcan catalyst synthesized at 0.1V vs.

RHE show a minor amount of Ag^0 due to AgO_2 layer formation on the surface, which may increase the electrocatalytic activity.

ORR polarization curves display the onset potential (Eonset) of Ag/Vulcan synthesized at 0.0 V, 0.1 V, 0.2 V, 0.3 V, and 0.4 V vs. RHE. **Figure 11** displays that the Eonset is kept almost constant in all Ag/ Vulcan catalysts, in which lower reduction potentials, up to 0.1 V, results in more positive ORR onset potentials. The Ag/Vulcan catalysts have a potential positive shift of 173, 126, 152, 163, and 186 mV, respectively, for catalysts prepared at 0.0 V, 0.1 V, 0.2 V, 0.3 V, and 0.4 V vs RHE. The potential shift is with respect to commercial Pt/ Vulcan (see **Table 5**). Moreover, the small size of these particles synthesized by the RoDSE technique and the high specific surface area provide more electrochemical active sites to carry out an efficient reaction.

For each electrocatalyst, mass activity was determined to elucidate electrocatalytic activity. In these calculations, all metal quantified by ICP-OES was active and accessible towards the ORR is assumed, shown in **Figure 11** for all Ag catalysts. Ag catalysts synthesized at 0.1 V showed the highest electrocatalytic activity based on mass activity. The ORR mass activities were 3,129 mA/mg, 4,765 mA/mg, 2,914 mA/mg, 4,313 mA/mg, and 1,637 mA/mg for 0.0 V, 0.1 V, 0.2 V, 0.3 V, and 0.4 V vs RHE, respectively. The most active catalyst (0.1 V) demonstrated three times higher activity than the least active one (0.4 V).

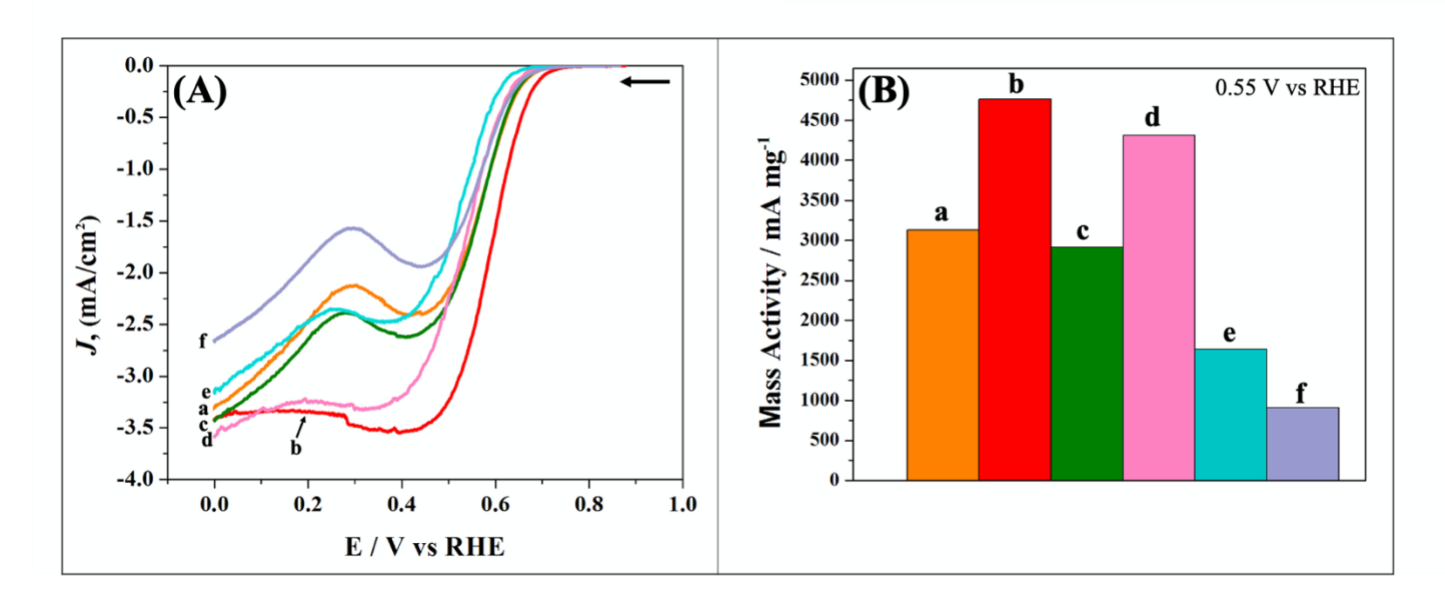


Figure 11. RDE polarization curves for ORR in O₂-saturated 0.1 M KOH solution at a scan rate of 5 mV/s at 1600 rpm (A) and (B) bar plot representation of ORR mass activity at 0.55 V vs. RHE for the following Ag/Vulcan in catalyst prepared at (a) 0.0 V, (b) 0.1 V, (c) 0.2 V, (d) 0.3 V, (e) 0.4 V and (f) 20% Ag/Carbon Vulcan vs. RHE.

In order to compare and evaluate the ORR kinetics on the electrodeposited Ag/Vulcan catalysts, RDE measurements were carried out at different electrode rotation rates and evaluated for ORR current densities using the Koutecky-Levich (K-L) equation, to determine the number of electrons (*n*) transferred, using the slope of the plotted points. The K-L plots are shown in Supporting Information Figure S4, and the corresponding n–E dependencies are shown in Figure S5. These catalysts mostly display a linear

relationship between the limiting current density and the rotation rate, which suggests first-order reaction kinetics towards the concentration of dissolved O₂ and similar numbers of *n* transferred for ORR at different reduction potentials applied. The potential is 0.55 V vs. RHE for all catalysts. From the slopes presented in **Figure S3**, the value of *n* (**Table 5**) per O₂ was slightly lower than four of the catalysts synthesized at 0.1 V and 0.3 V vs. RHE, calculated to be 3.5 and 3.4, respectively, which was similar to the commercial Pt/C, suggesting a dominant four electron reduction process. However, for Ag/Vulcan catalyst synthesized at 0.0 V, 0.2 V, and 0.4 V vs. RHE, exhibited low ORR activity, with a *n* value of 2.9, 2.8 and 2.7, respectively, which suggest that a few H₂O₂ is formed on this catalyst and the ORR proceed at least partially via series of 2 + 2 electron pathway. As mentioned earlier, for this study the RoDSE technique was used to synthesize our catalysts. With this technique, it is not necessary to add surfactants or any additive for the preparation of Ag/ Vulcan catalysts. For this reason, the value of *n* is lower in these reduction potentials, due to the amount of Ag catalyst on the substrate surface.

Table 5. Summary of ORR Activity for Ag/Vulcan catalysts synthesized at the different reduction potential and the benchmarks catalyst at 0.55 V vs. RHE

Sample	E _{onset} vs. RHE	E _{1/2} vs. RHE	n
$\mathbf{Ag}\ 0.0\ \mathbf{V}$	0.706	0.578	2.9
Ag 0.1 V	0.753	0.587	3.5
Ag 0.2 V	0.727	0.566	2.8
Ag 0.3 V	0.716	0.534	3.4
Ag 0.4 V	0.693	0.535	2.7
commercial 20% Ag/Vulcan	0.702	0.568	2.4
commercial 20% Pt/Vulcan	0.879	0.752	4.1

Conclusions

Vulcan XC-72R carbon-supported Ag/NPs electrocatalysts were successfully synthesized using the RoDSE method. This technique was used by applying five different Ag reduction potentials for the preparation of the Ag NPs supported on Vulcan XC-72R. The main purpose was to determine the ideal electrodeposition parameters that guarantee ideal metal loading and particle dispersion to carry on an efficient ORR through the 4e pathway. These catalysts were studied by XRD to demonstrate the presence of all of the expected peaks of Ag, indicating that Ag is mostly in its metallic form. Results from TEM and ICP-OES showed a strong relation between the applied electrodeposition potential, size of the Ag NPs and, Ag mass loading on the carbon support. In Raman spectroscopy, Ag on Vulcan synthesized at 0.2 V had a D band shift to higher frequencies and demonstrated more uniform distribution than the other Ag catalysts done at different reduction potentials. XPS results demonstrate that samples obtained by RoDSE at 0.1 V vs. RHE had the highest concentration of silver oxide (85%), while samples obtained at 0.2 V had the main concentration of metallic Ag (88%). Samples obtained at 0.4 V had an even distribution of Ag⁰ and Ag₂O species. Although the Ag 3d XPS binding energy peaks show that the Ag deposition on Vulcan XC-72R is affected by the electrodeposition potential, no trend as a function of the potential variation was observed.

From the ORRs results done by CV and RDE, the Ag/Vulcan catalyst were found to proceed in a combined pathway, mainly through a 2e⁻ pathway, for catalyst prepared at 0.0 V, 0.2 V and 0.4 V, and through a 4e⁻ pathway, for catalysts prepared at 0.1 and 0.3 V. The Ag/Vulcan catalyst synthesized in this work exhibited excellent ORR activity in alkaline solutions, which is superior to the commercial Ag/C catalyst. The results presented here suggest that that the deposition potential of Ag has an effect on the electrocatalytic behavior of the Ag/VulcanXC-72R. The synthesis performed at 0.1V vs. RHE showed slightly higher electrocatalytic activity towards ORR with a larger amount of oxides in its structure. In this work, the oxygencontaining carbon surface functional group and the Ag NPs suggest a synergistic effect in the ORR mechanism. Applying a RoDSE electrodeposition potential of 0.1V vs. RHE provided optimal conditions to generate Ag catalysts with low agglomeration, higher mass activity, and relatively small nanoparticles, which enabled an enhanced ORR via ca. 4e- process.

Acknowledgments

The authors express their gratitude to both the National Science Foundation NSF-PREM: Center for Interfacial Electrochemistry of Energy Materials (CiE²M) grant number DMR-1827622 and NSF-CREST Center for Innovation, Research and Education in Environmental Nanotechnology Grant Number HRD-1736093. APD acknowledges the NASA Fellowship from NASA Puerto Rico Space Grant Consortium No. NNX15AI11H. GSCQ was supported by the National Institute of Health under the MARC program, grant number 5T34GM007821-40. The use of the Cornell Center for Materials Research Shared Facilities, which is supported through the NSF MRSEC grant number DMR-1719875, is greatly appreciated.

Supporting Information Available: The following file is available free of charge. *SI Potential Dependent Ag Nanoparticle Electrodeposition on Vulcan XC-72R Carbon Support for Alkaline Oxygen Reduction Reaction.* The following information is included in this document: XPS, electrodeposition chronoamperometries, and ORR RDE data of the catalysts are presented.

REFERENCES:

- 1. R. Quadrelli, S. Peterson, The energy-climate challenge: Recent trends in CO₂ emissions from fuel combustion, Energy Policy 35 (2007) 5938-5952.
- 2. K. Caldeira, A.K. Jain, M.I. Hoffert, Climate Sensitivity Uncertainty and the Need for Energy Without CO₂ Emission, Science 299 (2003) 2052.
- 3. M. Bhattacharya, S.R. Paramati, I. Ozturk, S. Bhattacharya, The effect of renewable energy consumption on economic growth: Evidence from top 38 countries countries, Appl. Energy 162 (2016) 733-741.
- 4. H. Begum, M. Ahmed, S. Cho, S. Jeon, Freestanding palladium nanonetworks electrocatalyst for oxygen reduction reaction in fuel cells, Int. J. Hydrog. Energy 43 (2018) 229-238.
- 5. B. Y.S. Lin, D. Kirk, S. J. Thorpe, Performance of alkaline fuel cells: A possible future energy system?, J. Power Sources 161 (2006) 474-483.
- 6. S.-A. Park, E.-K. Lee, H. Song, Y.-T. Kim, Bifunctional enhancement of oxygen reduction reaction activity on Ag catalysts due to water activation on LaMnO₃ supports in alkaline media, Sci. Rep. **5** (2015) 13552.
- 7. M.S. Ahmed, H.S. Han, S. Jeon, One-step chemical reduction of graphene oxide with oligothiophene for improved electrocatalytic oxygen reduction reactions, Carbon 61 (2013) 164-172.
- 8. M. Vega-Cartagena, E.M. Flores-Vélez, G.S. Colón-Quintana, D.A. Blasini Pérez, M.A. De Jesús, C.R. Cabrera, Silver–Palladium Electrodeposition on Unsupported Vulcan XC-72R for Oxygen Reduction Reaction in Alkaline Media, ACS Applied Energy Materials ACS Appl. Energy Mater. 2 (2019) 4664–4673.
- C. Velez, J. Corchado-Garcia, A. Rojas-Pérez, E. J. Serrano-Alejandro, C. Santos-Homs, J. J. Soto-Pérez, C. Cabrera, Manufacture of Pd/Carbon Vulcan XC-72R Nanoflakes Catalysts for Ethanol Oxidation Reaction in Alkaline Media by RoDSE Method, J. Electrochem. Soc. 164 (2017) D1015-D1021.
- 10. E. Smirnov, P. Peljo, M.D. Scanlon, H.H. Girault, Interfacial Redox Catalysis on Gold Nanofilms at Soft Interfaces, ACS Nano 9 (2015) 6565-6575.
- 11. X. Wen, L. Bai, M. Li, J. Guan, Ultrafine iridium oxide supported on carbon nanotubes for efficient catalysis of oxygen evolution and oxygen reduction reactions, Mater. Today Energy 10 (2018) 153-160.
- 12. Y. Joo, M.S. Ahmed, H.S. Han, S. Jeon, Preparation of electrochemically reduced graphene oxide-based silver-cobalt alloy nanocatalysts for efficient oxygen reduction reaction, Int. J. Hydrog. Energy 42 (2017) 21751-21761.
- 13. J. Guo, A. Hsu, D. Chu, R. Chen, Improving Oxygen Reduction Reaction Activities on Carbon-Supported Ag Nanoparticles in Alkaline Solutions, J. Phys. Chem. C 114 (2010) 4324-4330.
- 14. D.A. Slanac, W.G. Hardin, K.P. Johnston, K.J. Stevenson, Atomic Ensemble and Electronic Effects in Ag-Rich AgPd Nanoalloy Catalysts for Oxygen Reduction in Alkaline Media, J. Am. Chem. Soc. 134 (2012) 9812-9819.
- 15. J. Mart Linge, H. Erikson, J. Kozlova, J. Aruväli, V. Sammelselg, K. Tammeveski, Oxygen reduction on electrodeposited silver catalysts in alkaline solution, J. Solid State Electrochem. 22 (1918) 81-89.
- 16. H. Erikson, A. Sarapuu, K. Tammeveski, Oxygen Reduction Reaction on Silver Catalysts in Alkaline Media: a Minireview, Chem. Electro. Chem. 6 (2019) 73-86.

- 17. J. Bañuelos, O. García, F. Rodriguez, L. Godínez, Electrochemically Prepared Iron-Modified Activated Carbon Electrodes for Their Application in Electro-Fenton and Photoelectro-Fenton Processes, J. Electrochem. Soc. 162 (2015) E154-E159.
- 18. E.C.-de Jesús, D. Santiago, G. Casillas, A. Mayoral, C. Magen, M. José-Yacaman, J. Li, C.R. Cabrera, Platinum Electrodeposition on Unsupported Single Wall Carbon Nanotubes and Its Application as Methane Sensing Material, J. Electrochem. Soc. 160 (2012) H98-H104.
- 19. D. Santiago, G. G. Rodriguez-Calero, H. Rivera, D. Tryk, M. Scibioh, C. Cabrera, Platinum Electrodeposition at High Surface Area Carbon Vulcan-XC-72R Material Using a Rotating Disk-Slurry Electrode Technique, J. Electrochem. Soc. 157 (2010) F189-F195.
- 20. M.A. Hernández-Rodríguez, M.C. Goya, M.C. Arévalo, J.L. Rodríguez, E. Pastor, Carbon supported Ag and Ag–Co catalysts tolerant to methanol and ethanol for the oxygen reduction reaction in alkaline media, Int. J. Hydrog. Energy 41 (2016) 19789-19798.
- 21. J. F. Moulder, W. F. Stickle, P.E. Sobol, K.D. Bomben, Handbook of X-ray Photoelectron Spectroscopy, Physical Electronics Division, Perkin-Elmer Corporation, 1992.
- 22. L. Betancourt, R. Guzman, S. Luo, D. J. Stacchiola, S. Senanayake, M. Guinel, C. Cabrera, Rotating Disk Slurry Au Electrodeposition at Unsupported Carbon Vulcan XC-72 and Ce³⁺ Impregnation for Ethanol Oxidation in Alkaline Media, Electrocatalysis 8 (2017) 87-94.
- 23. T. Jiao, H. Guo, Q. Zhang, Q. Peng, Y. Tang, X. Yan, B. Li, Reduced Graphene Oxide-Based Silver Nanoparticle-Containing Composite Hydrogel as Highly Efficient Dye Catalysts for Wastewater Treatment, Sci. Rep. 5 (2015) 11873.
- 24. M.S. Ahmed, S. Jeon, New functionalized graphene sheets for enhanced oxygen reduction as metal-free cathode electrocatalysts, J. Power Sources 218 (2012) 168-173.
- 25. M.-C. Hsiao, S.-H. Liao, M.-Y. Yen, P.-I. Liu, N.-W. Pu, C.-A. Wang, C.-C.M. Ma, Preparation of Covalently Functionalized Graphene Using Residual Oxygen-Containing Functional Groups, ACS Appl. Mater. Interfaces 2 (2010) 3092-3099.
- 26. M. Ahmed, D. Kim, S. Jeon, Covalently grafted platinum nanoparticles to multi walled carbon nanotubes for enhanced electrocatalytic oxygen reduction, Electrochim. Acta 92 (2013) 168–175.
- 27. M.S. Ahmed, S. Jeon, Electrochemical activity evaluation of chemically damaged carbon nanotube with palladium nanoparticles for ethanol oxidation, J. Power Sources 282 (2015) 479-488.
- 28. G. Socrates, Infrared and Raman Characteristic Group Frequencies: Tables and Charts, 3rd Edition, Wiley, 2004.
- 29. W. Chen, L. Yan, P.R. Bangal, Chemical Reduction of Graphene Oxide to Graphene by Sulfur-Containing Compounds, J. Phys. Chem. C 114 (2010) 19885-19890.
- 30. S. Pérez-Rodríguez, E. Pastor, M.J. Lázaro, Electrochemical behavior of the carbon black Vulcan XC-72R: Influence of the surface chemistry, Int. J. Hydrog. Energy 43 (2018) 7911-7922.
- 31. M.J. Lázaro, L. Calvillo, V. Celorrio, J. Pardo, S. Perathoner, R. Moliner, Study and application of Vulcan XC-72 in low temperature fuel cells, In Carbon Black: Production, Properties and Uses, Editors: I. J. Sanders, T. L. Peeten, Nova Science Publishers, Inc. 2011, Chapter 2.
- 32. C.-Y. Su, Y. Xu, W. Zhang, J. Zhao, X. Tang, C.-H. Tsai, L.-J. Li, Electrical and Spectroscopic Characterizations of Ultra-Large Reduced Graphene Oxide Monolayers, Chem. Mater. 21 (2009) 5674-5680.
- 33. X. Yang, L. Gan, C. Zhu, B. Lou, L. Han, J. Wang, E. Wang, A dramatic platform for oxygen reduction reaction based on silver nanoclusters, Chem. Commun. 50 (2014) 234-236.